Hindawi
Advances in Civil Engineering
Volume 2022, Article ID 2705691, 17 pages
https://doi.org/10.1155/2022/2705691

Research Article

Comparing Numerical Results for Seismic Performance of Portal Steel Frames Braced with Steel: HSS Brace, Glulam Timber Brace, and Timber-Steel-BRB

Saeed-Reza Sabbagh-Yazdi and Ainullah Mirzazadah

Civil Engineering Department, K. N. Toosi University of Technology, P.O. Box: 15875-4416, Tehran, Iran

Correspondence should be addressed to Ainullah Mirzazadah; ainullah.mirzazadah@email.kntu.ac.ir

Received 27 January 2022; Revised 6 May 2022; Accepted 10 June 2022; Published 20 July 2022

Academic Editor: Jorge Branco

This study involves the application of timber-based bracings elements. For this purpose, seismic analyses are performed on special portal steel frames without the brace and diagonally braced with Glued Laminated Timber (glulam) and Timber-Steel Buckling Restrained Brace (TS-BRB), and the results are compared with the same configuration using steel Hollow Structural Sections (HSS) bracing, using OpenSees structural analyzer. First, to verify the accuracy of the modeling, the numerical results are compared with experimental measurements on several types of elements: (a) diagonally braced frame with steel Hollow Structural Sections with a concentrically steel braced frame which was tested by the quasi-static method under cyclic loading protocol by previous researchers, (b) diagonally glulam braced frame with results of shake table tests on single-story timber braced frames, and (c) Timber-Steel Buckling Restrained Brace (TS-BRB) frame with experimental results of Heavy Timber Buckling-Restrained Braced Frame (HT-BRB). In the second step, the aforementioned timber base bracing alternatives (glulam, TS-BRB) are applied in the special portal steel frame, then the seismic performance of the frame is investigated under pushover, cyclic, time history, and incremental dynamic analysis (IDA), and then the results are compared with the behavior of similar portal frame in two conditions without the brace and diagonally braced with the steel-HSS brace. Results showed that steel-HSS, glulam, and timber-steel buckling restrained braces have significant roles in energy dissipation, increasing shear capacity, decreasing interstory drift, and decreasing weight and cost of estimation of the structure.

1. Introduction

Since experimental tests on steel frames are very time-consuming, numerical modeling is a suitable alternative to expensive laboratory tests, especially in the field of steel frame research. Nowadays, researchers have access to various software packages such as ABAQUS, ANSYS, and OpenSees. To understand the physical performance, many researchers have performed numerical modeling using OpenSees platforms. Seismic performance is described by designating the maximum allowable damage state for an identified earthquake ground motion. Performance objectives such as life safety, collapse prevention, and immediate occupancy are used to define the state of the building following a design earthquake. It is necessary to design steel frames to perform well under seismic loading. It has been observed that steel frames without bracing perform poorly in severe earthquakes. The seismic performance of steel frames can be improved by using different types of steel and wooden bracing. Steel braces have been used since ancient times and a lot of research has been done on them. Nowadays, researchers also use wood and hybrid wood-steel bracing for frames that performed poorly in severe earthquakes. Moore [1] reported details of the structural design of a 12-story studio building constructed in Auckland, New Zealand. The building's earthquake-resistant system consisted of traditional concentrically braced steel frames (CBF), while the floor system consisted of 65 mm thick glulam panels bonded to gypsum board. Gilbert et al. [2] proposed a hybrid system of glulam frames and buckling restrained steel braces (BRBs)

to avoid damage to the connections between timber members. The authors performed a nonlinear dynamic analysis (NLDA) on a plane model of a 6-story ideal building constructed with the new system and a moment-resisting steel frame. Gilbert et al. [3] proposed the integration of glulam frames with friction-reducing steel struts. The authors performed quasi-static and pseudodynamic unidirectional tests on a half-scale subassembly consisting of a wood beam-column connection and steel braces with friction dampers connected by a steel connection and glued-in bars. Timmers et al. [4] performed modal spectral analyses with numerical models for the hybrid timber structure, which consisted of steel-BRB braced chevron frames and glulam columns. The frame was designed to allow the BRBs to yield in tension and compression and dissipate seismic energy. Bracing may be provided to increase the response of the structure to lateral loading and to provide good ductility characteristics for good performance under seismic loading. Frame and braces form a vertical truss, and lateral loading is resisted by the action of the truss. The bracings allow the system to achieve a significant increase in lateral stiffness with minimal additional weight. As a result, they increase the natural frequency and usually reduce the lateral displacement. As a result of the inelastic effect of the bracing, they develop ductility. In the cyclic analysis under seismic loading, there is a deterioration in the strength of the structural members. These are significant properties of frame members under cyclic loading, which leads to a reduction in deformation capacity. Cyclic analysis is proposed to determine the seismic requirements for structures that consider the cumulative damage under cyclic loading. In seismically active regions, it is generally not economically feasible to design conventional structures to remain resilient during severe earthquake motions. Fortunately, this may not be necessary if it is possible to take advantage of the ability of several types of structures to dissipate energy through inelastic action. In addition, fragility curves play an important role in estimating the vulnerability of structures. Seismic fragility of structures describes the probability of damage due to random ground motions. An alternative is to use analytical methods such as incremental dynamic analysis (IDA) to develop the fragility curves for different structures. Pushover analysis is an analysis method in which the structure is under lateral force with an invariant height distribution until the target displacement is reached. The displacement is plotted with the base shear to obtain the static pushover curve. With the help of pushover analysis, we obtain the shear capacity of the structure and this analysis helps us to determine the formation of the first plastic hinge, according to which we can study the behavior of the structure after the formation of the first plastic hinge. For design or evaluation purposes, the seismic capacity of the structural system for different seismic hazard levels can be calculated by nonlinear time history analysis using several properly selected ground motions. Ground motion selection plays a crucial role in seismic analysis. This study is divided into three steps: In the first step, the macro element modeling approach using OpenSees of portal steel frames is presented, and details of various simulations are discussed. In the second step, the models are studied under pushover, cyclic, time history, and IDA analyses. In the third step, the results are discussed and concluded. The purpose of this analysis was to compare the capacity curves before and after bracing and also to compare the hysteresis curves which show earthquake energy dissipation and to reduce the maximum interstory drift by using different types of timber base bracing.

Table 1: Glulam brace mechanical property [5].

Modulus of elasticity (MPa)	Shear modulus (MPa)	Poisson ratio
$E_R = E_3 = 949$	$G_{RT} = G_{32} = 119.3$	$V_{LR} = V_{13} = 0.331$
$E_T = E_2 = 488$	$G_{LR} = G_{13} = 819$	$V_{LT} = V_{12} = 0.406$
$E_L = E_1 = 10844$	$G_{LT} = G_{12} = 656$	$V_{RT} = V_{32} = 0.6$
		$V_{TR} = V_{23} = 0.331$
		$V_{RL} = V_{31} = 0.037$

2. Numerical Modeling Framework

The modeling approach of portal steel frames in OpenSees has presented four portal steel frames in this section: portal steel frame without bracing, portal steel frame with bracing of glulam, portal steel frame with bracing of hollow steel sections (HSS), and portal steel frame with bracing of hybrid wood-steel buckling braces (TS-BRB). Details of the specimens and material properties are given in Tables 1–3, respectively.

Three types of braces have been used. The first type of brace has a hollow steel cross section and the second type of the brace is a hybrid buckling restrained brace with a steel core confined by glulam timber as shown in Figures 1 and 2, and the third type is an ordinary glulam brace whose section is shown in Figure3. In hybrid timber-steel buckling restrained brace (TS-BRB) screws mechanically strengthen the brace assembly together, glulam timber casing is to resist global buckling, and the steel core plate at the unboned internal interfaces is to resist higher mode buckling; final assembly of the specimens consisted of mechanically laminating the glulam and steel core plate assembly together with 3/8 in (9.5 mm) diameter fully high tensile strength screws. The dimensions of the groove in each section of the glulam casing that houses the core plate required a tight control on tolerances. To obtain this, the glulam specimens were made on a five-axis CNC mill that achieved a tolerance of 0.04 in (1 mm) in both depth and width of the groove. The main central plate is cut to its profiled shape using a CNC plasma cutter. The cut main plate has to be free of notches and defects, and, within the yielding core, length has a surface roughness not-to-exceed 1000 μin (25.4 μ) [6].

2.1. FEM Modeling. OpenSees is capable of simulating the response of structural systems subjected to earthquakes via FEM. In OpenSees, structural elements can be introduced at the element level, sectional level, and fiber level by introducing different relations, force-axial strain/moment-curvature

Table 2: Frames members material mechanical Property.

Type of frames	Members	Fy (MPa)	Modulus of elasticity (MPa)
Steel-HSS braced frame	Beams and columns	275	200000
	Steel brace	275	200000
	Gusset plates	275	200000
Unbraced Frame	Beams and columns	275	200000
Glulam braced frame	Beams and columns	275	200000
	Gusset plates	275	200000
Timber-steel-BRB	Brace core	248	200000

Table 3: Details of the frame and brace specimens.

Specimen	Material	Section (mm)	A (mm^2)
Frames columns	Steel	IPE200	2850
Frames beam	Steel	IPE200	2850
Timber base brace	Glulam	(100×100)	10000
Steel-HSS brace	Steel	HSS $(60 \times 60 \times 3)$	674
TS-BRB core	Steel	(50×20)	1000

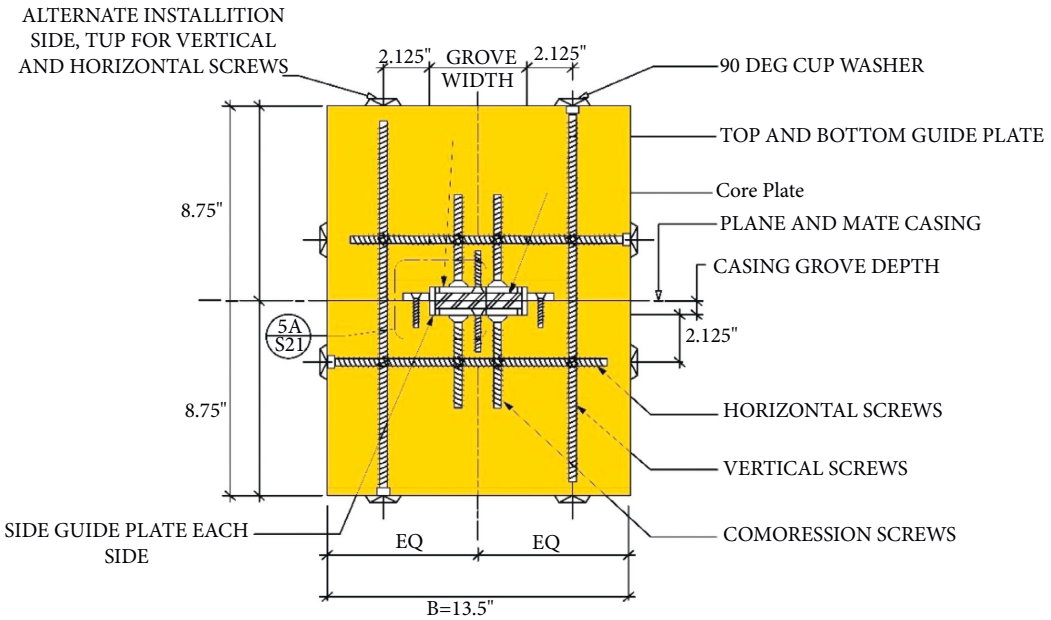

Figure 1: TS-BRB section details.

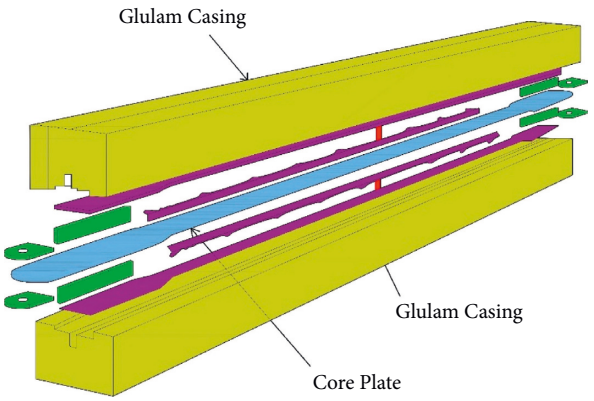

Figure 2: Exploded view TS-BRB.

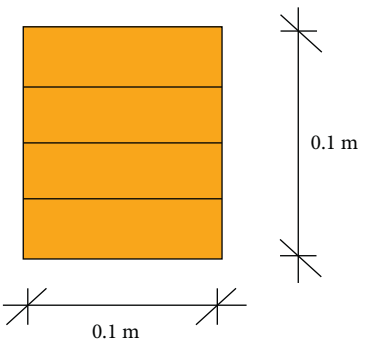

Figure 3: Glulam brace section.

relations, and stress-strain curves, respectively. In the following, the various macroelement modeling steps of the special portal steel frame in OpenSees are described. Here are two general numerical methods for the investigation of the nonlinear behavior of special portal frame members in OpenSees: The first one is to use concentrated plasticity by zero length elements which work as rotational springs to represent the structure's nonlinear behavior as shown in Figure 4. The rotational springs capture the nonlinear behavior of the frame; the springs employ a bilinear hysteretic response based on the modified Ibarra-Krawinkler deterioration model. The second approach is to use distributed plasticity as shown in Figure 5. In this method, the plasticity is distributed over a defined length. The related responses of each plastic hinge area are defined as separate sections. The axial response is specified by an elastic section, while the flexural response is defined by a uniaxial section using two-line material based on the modified Ibarra-Krawinkler model. The rotational performance of the plastic hinges in models follows hysterical response based on the updated Krawinkler model [7], which is derived from an extensive database of steel component tests. Alternatively, these input parameters can be determined using approaches similar to those described in FEMA 356.

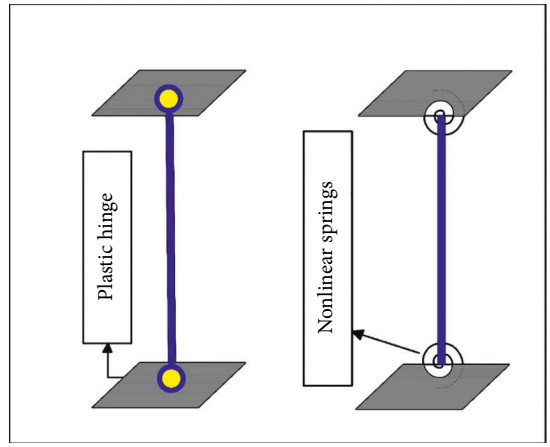

Figure 4: Concentrated plasticity models.

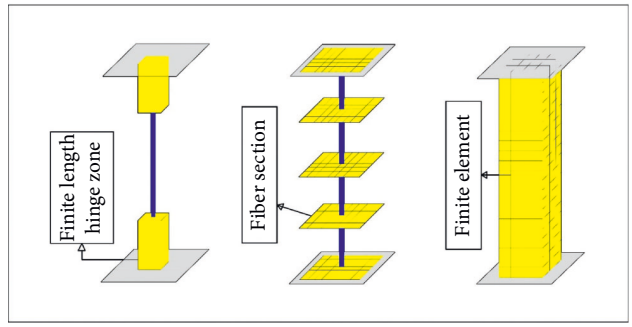

Figure 5: Distributed plasticity models.

2.1.1. FEM Modeling of Timber-Based Glulam Bracing. The model in this study is a single-story special portal steel frame, braced with a timber based glulam brace. In this study, first the beam and columns nonlinear behavior is represented using the concept where the plastic behavior occurs over a finite length. The brace's nonlinear behavior is represented using the concentrated plasticity concept with rotational springs. The models are assumed to be located in Tehran according to the earthquake zoning map of Iran, in a region with relatively high risk, and the ground acceleration of the earthquake is 0.35 in soil type C. In models, the width of the frame is 8 meters, and the height of the frame is 4.5 meters as shown in Figure 6. Criteria of analysis and design were considered by ASCE-7 with the requirements of FEMA P-695. The modeling of the gusset plates was performed using the rotational hinge method introduced by Po-Chien Hsiao et al. [8]; in the proposed method, the connections of the beams to the column are considered moment-resistant and, at the end of the beams, the top and bottom of the columns, and also at the two ends of the brace, rigid offsets (elastic element with high stiffness) are introduced. These rigid areas at the end of the members are then connected to the main members by rotational springs as shown in Figure 7. The connections of the columns to the foundation are rigid. Simulations were performed using OpenSees software for modeling of the beams and columns, and the nonlinear beam-column element with the plasticity in the length of element (with five integration points along the element) and fiber cross section were used. In the models, the effect of the dead and live loads are nodal masses at the joint of beams and columns mx = 2250 kg for nodes 3 and 4.

All analyses are performed in two dimensions in OpenSees model for analysis which is shown in Figure 8. The

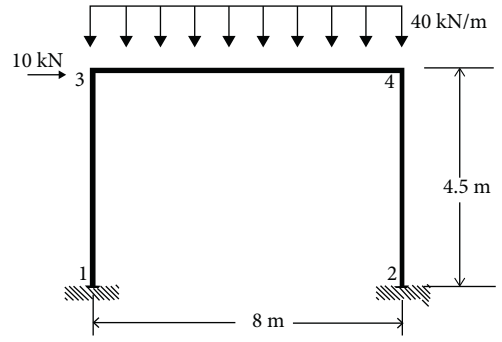

Figure 6: Gravity static loading for gravity analysis.

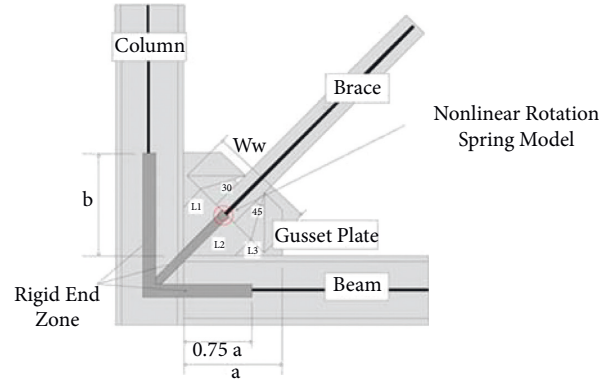

Figure 7: Brace connection model.

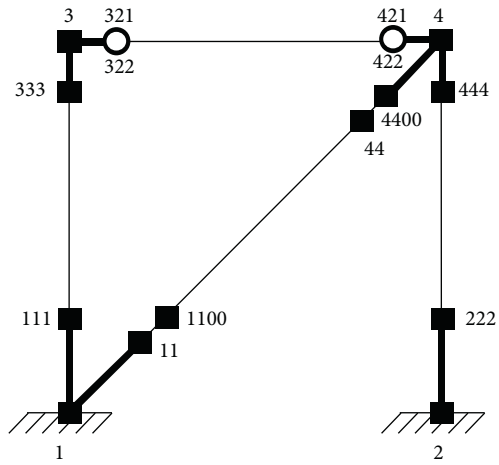

Figure 8: OpenSees model for analysis.

frame is analyzed under gravity loads before the pushover, cyclic, time history, and IDA analysis are conducted. For modeling glulam brace in OpenSees elastic elements with uniaxial material elastic are used [9].

2.1.2. FEM Modeling of Timber-Steel-BRB Bracing. For special portal steel frame, braced with timber-steel buckling restrained brace (TS-BRB), the beams, columns, and connections are modeled as mentioned in glulam bracing; the conditions of frames are the same, and the only difference is in braces; the core of timber-steel-BRB is made of steel (50×20 mm) and confined by glulam to resist global buckling of core. Beams and columns are modeled by nonlinear beam-column command with fiber sections. Rigid offsets were used at the beam-column intersection and brace to frame connections to model the gusset plates. BRBs were modeled with a corotational truss command with yielding steel core area. Since a single truss element was used for the whole brace, the equivalent elastic modulus was used to model the yielding and the nonyielding section of the brace. According to the research of Atlain Ozgur et al. [10], the TS-BRB was modeled using a Corotational Truss Element. Corotational Truss Element command is used to construct a Corotational Truss. Corotational rules accept a set of corotational axes which rotate with the element, thus taking into computation an exact geometric change between local and global frames of reference. Brace adjusted strength can be obtained from the following equation.

$$P_{ysc\,(\text{adjusted})} = \omega.\beta.A_{sc}.F_{ysc}, \tag{1}$$

where ω is the strain hardening adjustment factor, β is the compression-strength adjustment factor, A_{sc} is the cross-sectional area of the yielding core, and F_{ysc} is yield strength of the steel core. These factors are mathematically represented as follows:

$$\beta = \frac{P_{\max}}{T_{\max}}, \qquad \omega = \frac{T_{\max}}{A_{sc}.F_{ysc}}, \tag{2}$$

where $T_{\max}$ is the maximum force (from testing) within deformations corresponding to two times the design story drift and $P_{\max}$ is measured maximum compression force (from testing).

3. OpenSees Modeling Verification

OpenSees needs to be verified before complex analyses are proceeded to check that the program is providing accurate results and to verify modeling practices for structural behavior. The models used for verification serve the purpose of proving program accuracy as well as usage for achieving desired dynamic structural behavior. Confirmation of OpenSees is essential because it ensures that the results will be dependable and valid in more complex analyses.

3.1. Steel-HSS Braced Frame Verification. To evaluate the accuracy of the modeling process of the steel-HSS braced frame, a two-story braced frame, where specimen and testing configurations are shown in Figure 9, tested by Lai et al. [11], is investigated under cyclic analysis in two dimensions using OpenSees finite element software; specimens specifications are listed in Table 4. Comparison of experimental and numerical results by OpenSees is shown in Figure 10. It is observed that the numerical results are in agreement with the experimental results.

3.2. Timber-Steel-BRB Frame Verification. The frame under study in Figure 11 is to perform verification of TS-BRB cyclic algorithms which is related to the article of Eric Ko et al. [6], which is a single-story steel frame equipped with TS-BRB glulam casing. The following figures show the details and dimensions of the relevant model.

Cyclic analysis was performed in two dimensions using OpenSees finite element software. The width and the height of the frame were assumed to be 4.19 m. The floor mass was allocated as a nodal mass at the intersection of beams and columns. This mass was assigned only for the X degree of freedom to activate the higher modes of the structure, and negligible masses of 1e-9 were also assigned to the second and third degrees of freedom. Frame connections to the foundation were considered rigid. The yield strength and modulus of elasticity of the steel used for the beams and columns were 275 MPa and 200 GPa, respectively, and their behavior was introduced as uniaxial material using the steel02 command in OpenSees. All local coordinate conversions (hardness transfer and element strength) were performed in Appendix software using the P-Delta option in the geometric transfer command. This command is used to construct a linear coordinate conversion that transfers the stiffness and strength of the elements from a local system to a global coordinate system by performing a linear geometric transformation considering the effects of the second P-Delta. The beam is W-shaped in dimensions of 0.2×0.1 m. The dimensions of the box columns were $0.457 \times 0.457 \times 0.012$ m. For modeling beams and columns, a nonlinear column beam element with distributed plasticity with five integration points along the element was used. The

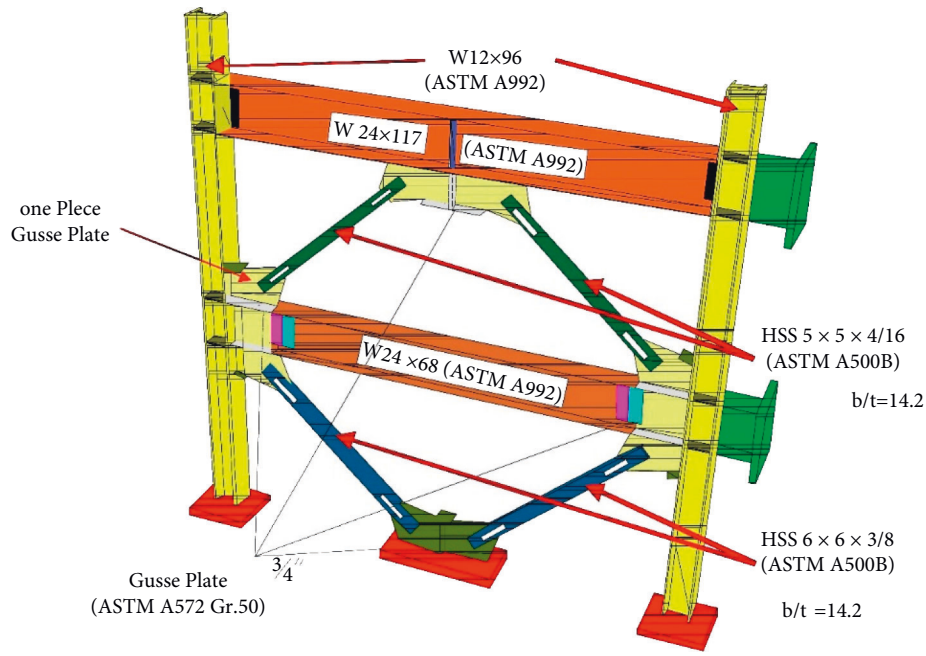

Figure 9: Specimen TCBF-B-1: member sizes [11].

Table 4: Name, member size, material type, and test method of the specimens [11].

Name	Column and beam	Brace	Test method
TCBF-B-1	W12 × 96 (columns and beams (ASTM A992))	HSS 5 × 5 × 5/16 HSS 6 × 6 × 3/8	Cyclic loading

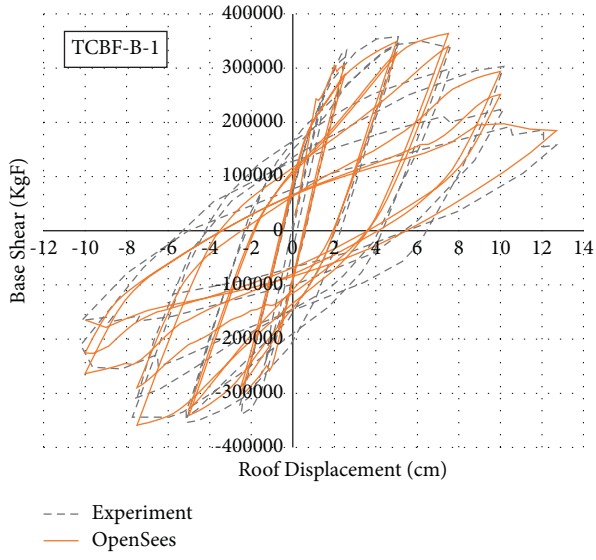

Figure 10: Experimental and numerical validation.

yield strength and modulus of elasticity of the steel used for the steel core of the TS-BRB brace are 248 MPa and 200 GPa, respectively, and their behavior was introduced as uniaxial material using the steel02 command in OpenSees. This is a rectangular steel core with an area of 1548 mm^2. In OpenSees software, for modeling the TS-BRB brace CorotTruss command was used. Figure 12 shows the validation result of the cyclic solution algorithm performed in OpenSees finite element software. The vertical and horizontal axes are the axial resistive force of the brace (KN) and the deformation of the brace joint with the gusset plate in the direction of the length of the brace, respectively. As can be seen, the curves have a good and acceptable fit.

3.3. Glulam Braced Frame Verification. To perform verification of glulam braced frame, the tested frame in Figure 13 was selected; the tested frame contains two planar four-hinged steel frames located parallel to each other 1.2 m apart. The two planar frames were attached with cross beams as well as with diagonal steel cross braces to supply the out-of-plane stiffness. The four-hinged steel frame was designed to supply vertical support for an inertial mass consisting of three concrete blocks attached to the top of the frame. The three concrete blocks had a total mass of 4500 kg (10000 lb). The frame itself has no lateral resistance, so the inertial forces are transmitted directly to the component tested, which in this case was the diagonal timber brace with connections on both ends. A photograph of the frame with the timber brace member inserted and ready for testing is shown. One of the crossbeams of the frame near the top was designed to assist the diagonal brace element intended for testing. The brace was held at the bottom by a specially designed fixture that was attached to the specimen attachment beam. Load cell was attached at the top end of the brace to directly compute the axial load induced in the member. Rotational pins were used on both ends of the brace to prevent the progress of bending moments on the brace. Because of the weight of the

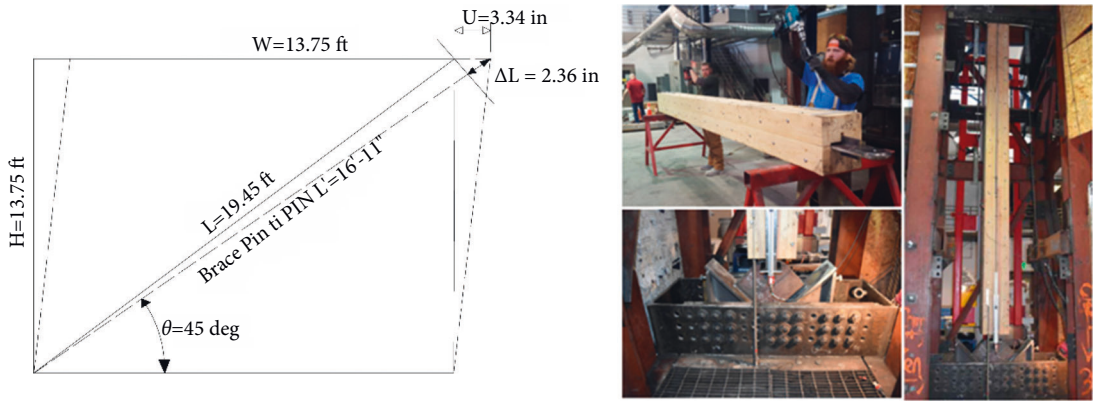

Figure 11: Tested timber-steel buckling restrained brace for verification [6].

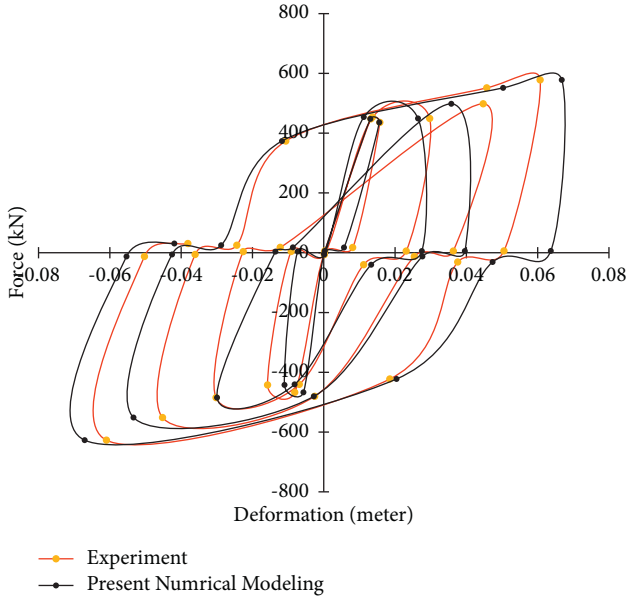

Figure 12: Cyclic experimental and numerical results of the TS-BRB frame.

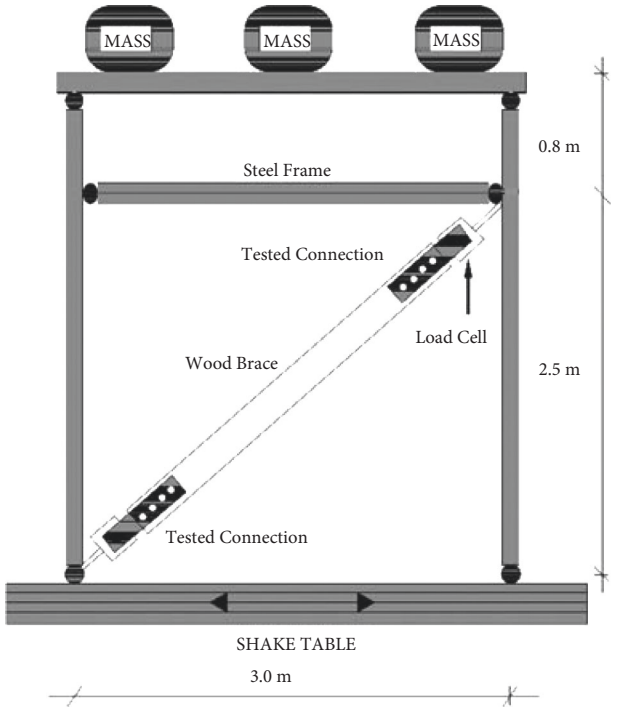

Figure 13: Test setup for the shake table tests [12].

setup at the top of the diagonal brace (fixture plus a load cell), rollers were attached to avoid out-of-line displacements of the brace that would cause rotation in the connection. The diagonal braces used in the tests consisted of spruce-pine (SP) Glued Laminated Timber (130 × 152 mm) in cross section. Brace specimens were approximately 3.1 m long and had the same connection on both ends. The average modulus of elasticity of glulam is 10844 MPa (1572.8 × 103 psi), time history analysis was performed using OpenSees finite element software under Joshua earthquake, and acceleration histories of the top frame were found and there was an acceptable fit to the shake table acceleration history (see Figure 14).

4. Seismic Analyses Strategies

Seismic performance of structural elements under seismic loading requires extensive research. Several research bodies all over the world have been interested in investigating the

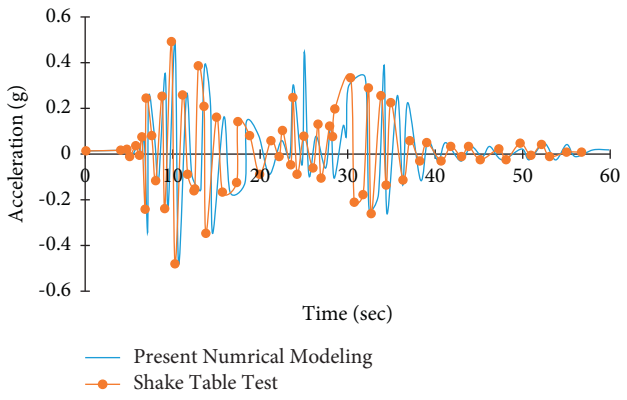

Figure 14: Acceleration history of the top frame.

seismic response of various types of structural systems. In general, research on the seismic performance of structural systems can be categorized into two groups: analytical investigation and experimental research. Because of innovation in the fields of electronics and mechanics, the progress of those two groups of research has been important. At present, simulating the static and dynamic earthquake responses of complex structural systems is not very difficult. Seismic analysis is a tool for estimating the response of structures in the process of designing earthquake-resistant structures or vulnerable structures. In principle, the problem is difficult because the structural response to severe earthquakes is dynamic, nonlinear, and random.

4.1. Pushover Curves of Selected Portal Frames. In pushover analysis, the load is applied in one direction to the structure. In this method, the lateral load is applied statically and gradually to the structure until the target displacement or the structure collapses [13]. In this study, the target displacement is calculated as 0.9 m. The displacement increment is taken as 0.01. FEMA-440 documents will propose several improvements to the basic displacement modification procedure. In FEMA-356 [13], these relate to the coefficient method equation for the target displacement (δ_t):

$$\delta_t = C_0 C_1 C_2 C_3 S_a \frac{T_e^2}{4\pi^2} g, \tag{3}$$

where T_e is the effective fundamental period of the structure in the direction under consideration, S_a is response spectrum acceleration at the effective fundamental vibration period and damping ratio of the structure under consideration, g is the acceleration due to gravity, C_0 is the modification factor that relates the elastic response of an SDF system to the elastic displacement of the MDF structure at the control node, C_1 is modification factor that relates the maximum inelastic and elastic displacement of the SDF system, C_2 is modification factor to represent the effects of pinched hysteretic shape, stiffness degradation, and strength deterioration, and C_3 is the modification factor to represent increased displacement due to P-Delta effects. Nonlinear static analysis can be performed in complete and simplified ways. In the complete method, the main and nonmain members are included in the model and their nonlinear behavior is selected as close to reality as possible. In the simplified method, only the main members are modeled. The nonlinear behavior of the principal members is simulated by a two-line model and the reduction effects are ignored [14]. The structure is subjected to a lateral load distributed across the height of the structure based on the following formula specified in FEMA-356 [14]:

$$F_X = \frac{W_X h_x^K}{\sum_{i=1}^{N} W_i h_i^K} V. \tag{4}$$

In the above equation, F_x is the applied lateral force at level "x," W is the story weight, h is the story height, and V is the design base shear. K is set equal to unity in an inverted triangular distribution of the lateral load. In this study, the portal steel frame is analyzed under pushover loading in four conditions: without bracing, steel-HSS braced, timber based glulam braced, and timber-steel buckling restrained braced (TS-BRB); their pushover capacity curves are shown.

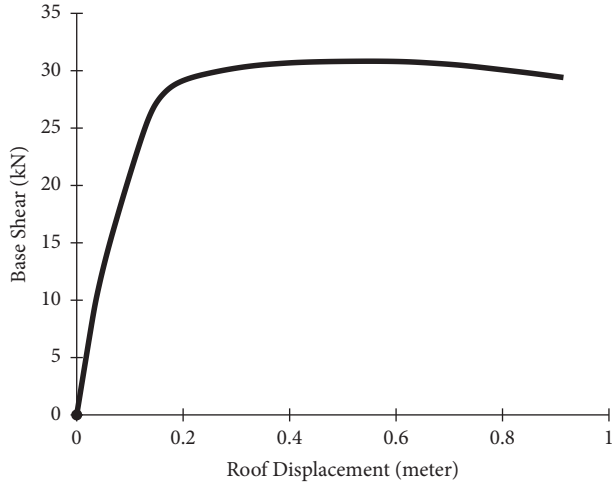

Figure 15: Unbraced portal frame pushover curve.

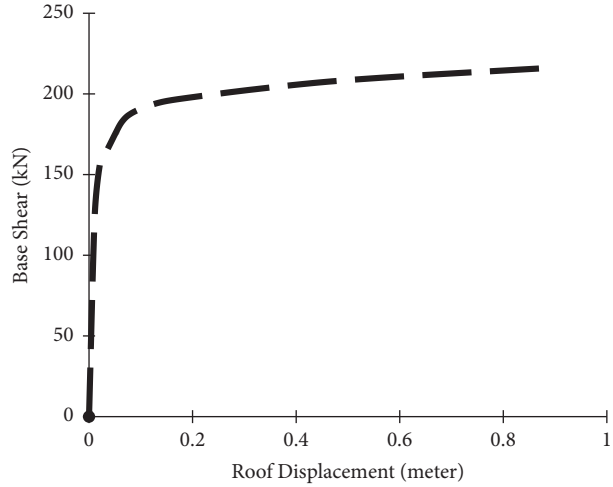

Figure 16: Steel-HSS braced portal frame pushover curve.

According to the results of pushover analysis, as shown in Figures 15–18, the portal steel frame without bracing has the lowest shear capacity. The slope of the elastic part of the capacity curve in the frame braced with the glulam brace is less than the slope of the frame braced with steel-HSS and TS-BRB braces; this means that the elastic stiffness of the frame braced with a glulam brace is less than the elastic stiffness of the frame braced with the steel-HSS and TS-BRB. The portal steel frame without bracing has the lowest values of elastic stiffness and seismic capacity, and even the slope of the part after the submission of the pushover curve is less than the frames braced with steel-HSS, timber based glulam, and TS-BRB. Comparative results of capacity curves of steel-HSS braced frames and frame braced with timber-steel buckling restrained brace (TS-BRB) show that the elastic stiffnesses (slope of the elastic region of the capacity curve)

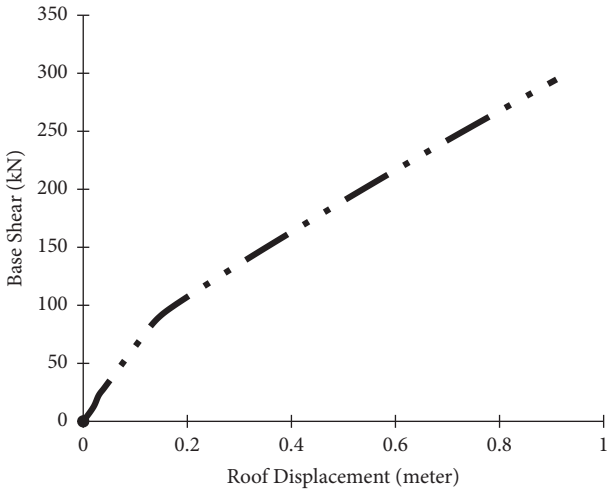

Figure 17: Glulam braced portal frame pushover curve.

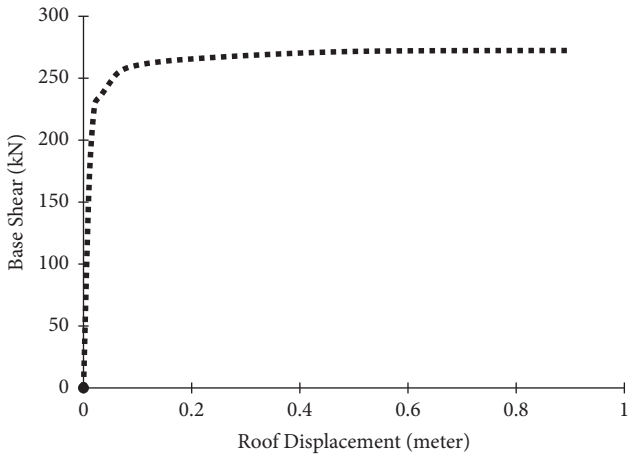

Figure 18: TS-BRB portal frame pushover curve.

of the two types of braces are almost the same, but the shear values and the total capacity of the TS-BRB braced frame are more compared to the frame braced with the steel-HSS. This indicates that, in the details and dimensions of the same design sections (equal hardness), the frame braced with TS-BRB has better performance and more capacity than the frame braced with the steel-HSS. Comparisons of base shear equivalent to the first plastic hinge formation and displacement values of frames are listed in Table 5.

4.2. Strength and Stiffness Degradation Investigation of Selected Portal Frames. In cyclic analysis, cyclic loading is applied to the structure and the effects of capacity reduction during cyclic loading can be observed. The result of cyclic loading is usually the curves of the force against the displacement from which the seismic performance of the studied members can be better achieved [15]; the greater the area below these curves, the more energy dissipation. On the other hand, resistance drop should not occur in high cycles. To apply cyclic loading, standard protocols such as ATC-24 standard [16] and SAC standard protocol [17] should be used. In this study, the portal steel frame is analyzed under cyclic loading with a displacement loop of 4 m in four conditions: without bracing, braced with steel-HSS, braced with timber based glulam, and braced with timber-steel buckling restrained brace (TS-BRB); its hysteresis curves are obtained as follows.

According to the results of cyclic analysis, as shown in Figures 19–22, the unbraced portal frame has the lowest energy dissipation area and has strength and stiffness degradation. The area under the cyclic curve of the frame indicates the energy dissipation; in the case of using the steel-HSS brace, the number of cycles is much higher and there is no drop in strength and stiffness in the higher cycles. As a result, in a portal steel frame, the use of a steel-HSS brace is preferable. According to the results in Figure 22, the frame braced with timber-steel buckling restrained bracing (TS-BRB) is slightly harder than the frame braced with the steel-HSS brace, and the number of reciprocating cycles in both frames is almost the same, but the area under the cyclic curve of the frame braced with TS-BRB is more than that of the frame braced with the steel-HSS brace; the TS-BRB braced frame can resist base shear in tension; the reason for these advantages is that the TS-BRB brace does not buckle under compression, and, as a result, the axial tensile and compressive capacities are almost equal. Therefore, according to the results, the best performance is related to frame braced with timber-steel buckling restrained brace (TS-BRB). Using timber based glulam, steel-HSS, and TS-BRB braces can remove strength and stiffness degradation as shown in Table 6.

4.3. Drift Investigation of Selected Portal Frames. Incremental dynamic analysis is one of the new methods in performance-based earthquake engineering, which expresses the behavior of the structure in a wide range of different earthquake intensities. Also, due to the dynamic nature of this method, we can certainly see more realistic results compared to nonlinear static methods. The method is based on the fact that to control the structure is analyzed for several or a single record of earthquake acceleration to obtain several points. By drawing and connecting these points, a continuous picture of the spectrum of the behavior of the structure in all elastic stages to yield and finally the collapse of the structure is obtained and finally show a good view of the newest methods in performance [18]. This method has been adopted by the US Federal Emergency Management Agency (FEMA) and has been considered in the FEMA-350, FEMA-351, and HAZUS-MH MR-5 guides to determine the overall failure capacity of the structure; IDA involves performing multiple nonlinear dynamic analyses of a structural model under a suite of ground motion records [18]. Some fundamental parameters of the IDA analysis used in this paper are defined as follows.

4.3.1. Selected Scale Factor (SF). Scale factor of an accelerogram, a_λ, is the positive scalar $\lambda \in [0; +\infty)$ [19] that produces a_λ when multiplicatively applied to the unscaled acceleration time history a_1:

$$a_\lambda = \lambda * a_1. \quad (5)$$

Table 5: Summery of base shear equivalent to the first plastic hinge formation of different frames.

Type of portal steel frame	First plastic hinge base shear (KN)	First plastic hinge point (m)	Brace effective area dimensions (mm)	Unit weight of brace length (Kg/m)
Steel-HSS Braced	171	0.019	HSS $(60 \times 60 \times 3)$	5.18
TS-BRB	222	0.019	(50×20)	7.85
Glulam braced	63	0.082	(100×100)	4.5
Unbraced portal	28	0.174		

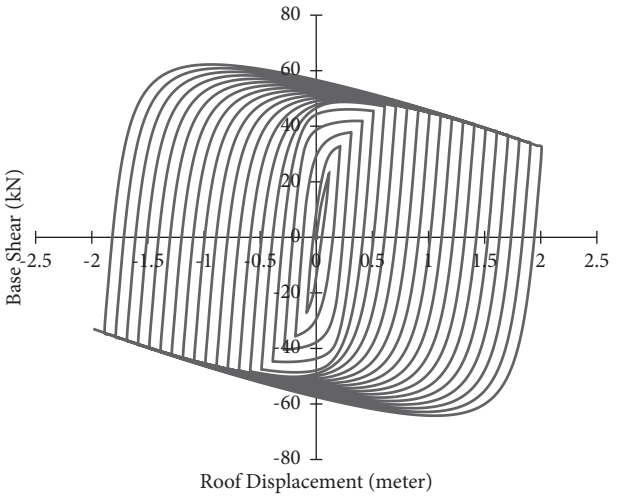

Figure 19: Unbraced portal frame hysteresis curve.

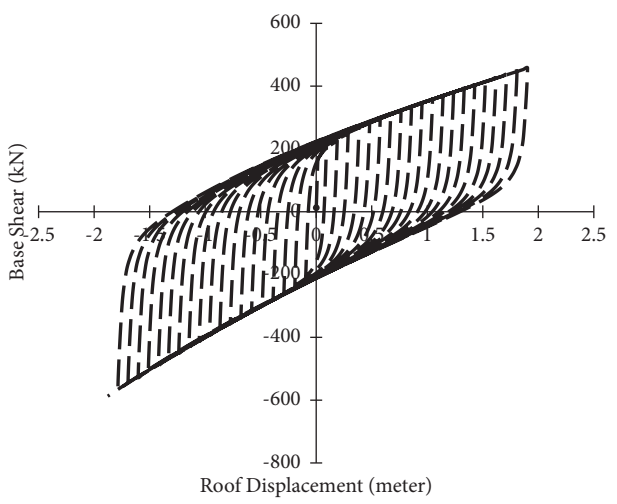

Figure 20: Steel-HSS braced portal frame hysteresis curve.

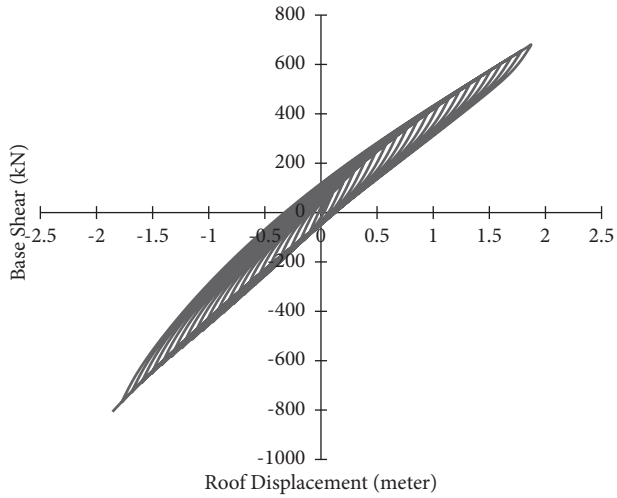

Figure 21: Glulam braced portal frame hysteresis curve.

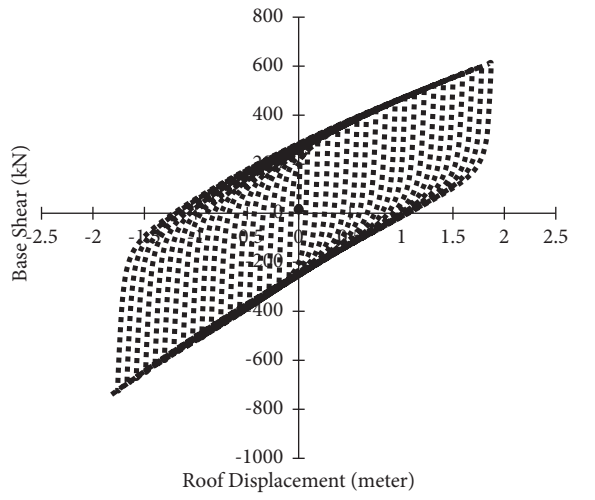

Figure 22: TS-BRB portal frame hysteresis curve.

The scale factor constitutes one-to-one mapping from the original to all its scaled pictures. Value of $\lambda = 1$ signifies the natural accelerogram, and $\lambda < 1$ is a scaled-down accelerogram, while $\lambda > 1$ corresponds to a scaled-up one. Scale factor is the easy way to determine the scaled images of an accelerogram.

4.3.2. Selected Intensity Measure (IM). The intensity measure depends on the unscaled accelerogram, a_1, and is monotonically increasing with the scale factor, λ. Several quantities are suggested to characterize the "intensity" of a ground motion record, such as peak ground acceleration and peak ground velocity. In this paper, the intensity measure is equal to the spectral acceleration corresponding to the first model of the structure with 5% damping Sa (T1, 5%).

$$IM = f(a_1, \lambda). \tag{6}$$

4.3.3. Selected Damage Measure (DM). Damage measure is positive scalar DM $\in [0; +\infty]$ that determines the additional

Table 6: Strength and stiffness degradation of braced and unbraced portal frames.

Type of portal steel frame	Brace effective area dimensions (mm)	Strength degradation	Stiffness degradation
Steel-HSS braced	HSS $(60 \times 60 \times 3)$	No	No
TS-BRB	(50×20)	No	No
Glulam braced	(100×100)	No	No
Unbraced frame		Yes	Yes

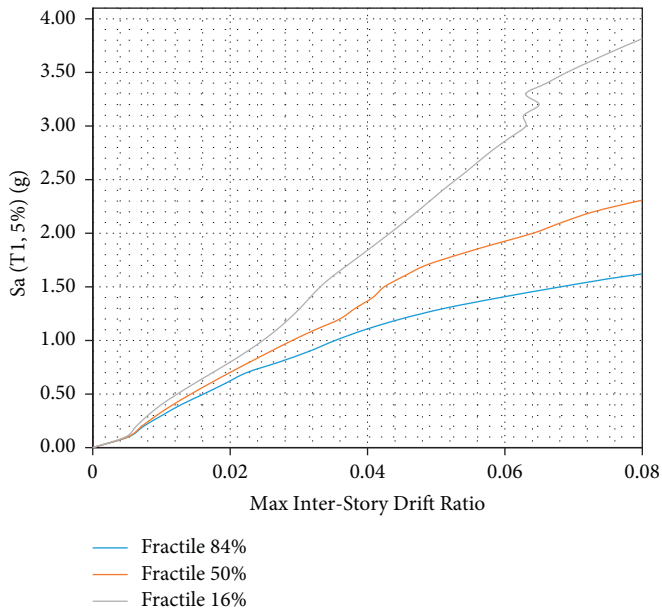

Figure 23: Fractile curves of the unbraced portal frame.

response of the structural model due to a prescribed earthquake loading. In other words, a damage measure is an observable quantity that is part of, or can be deduced from, the output of the corresponding nonlinear dynamic analysis. In this paper, the maximum interstory drift is selected seismic damage measure [19].

4.3.4. Summarized IDA or Fractile Curves. After performing IDA analysis under several different earthquake records, a set of IDA curves are obtained. Given a large number of curves, each of which shows the specific behavior of the structure under the earthquake records and does not indicate the overall performance of the structure in the case of earthquake types; to achieve a general state of structural behavior and reduce information scatter, the category of IDA curves can be summarized [20]. This is possible through statistical methods and, in this method, the performance of the studied structures can be evaluated more tangibly. Therefore, three statistical values of 16%, 50%, and 84% are extracted from each of the categories of IDA curves and they are used to compare different categories of curves with each other and evaluate the probabilities of structures. In this paper, the portal steel frame is IDA analyzed in four conditions: without bracing, braced with steel-HSS, braced with timber based glulam, and braced with timber-steel buckling restrained brace (TS-BRB). Summarized IDA or fractile curves are shown in Figures 23–30.

4.4. Selected Performance Level. In this study, the immediate occupancy (IO) capacity of the frames is compared under selected earthquake records. Immediate occupancy performance level corresponds to a small reduction in lateral stiffness and strength or the structure substantially retains original strength and stiffness, minor cracking of facades, partitions, ceilings, and structural elements can be restarted.

4.5. Limit States on IDA Curves. For performance calculations, limit states on the IDA will be defined as listed in Table 7. Three commonly used limit states are considered, namely, immediate occupancy, collapse prevention (as per FEMA [21]), and global dynamic instability. For the models in this paper, immediate occupancy is defined according to FEMA guidelines [21]. The immediate occupancy limit state is defined at $\theta_{\max} = 1\%$ for ordinary moment frame and $\theta_{\max} = 2\%$ for special moment frame.

4.6. Research on Near-Fault Earthquakes. In areas near the fault, ground movements are influenced by the fracture mechanism, the direction of fault expansion is related to the site, and the permanent displacement of the ground is due to the static slide of the fault. However, a single distance is not defined as a close range of the fault, and there is a difference of opinion among researchers in this regard. For this reason, researchers have suggested different distances between 10

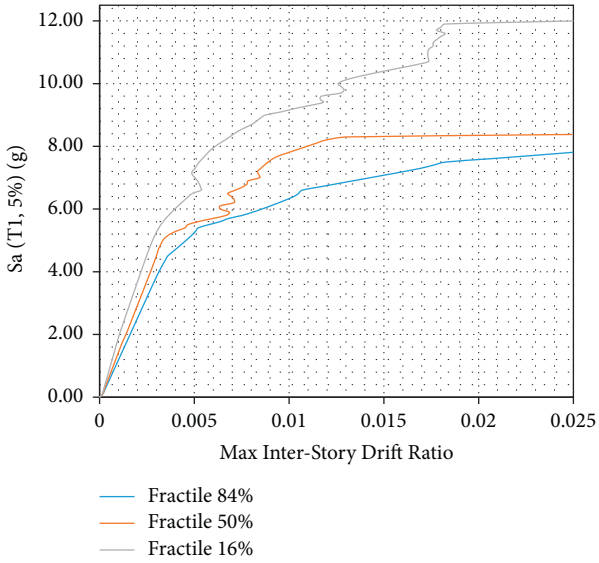

Figure 24: Fractile curves of the TS-BRB braced portal frame.

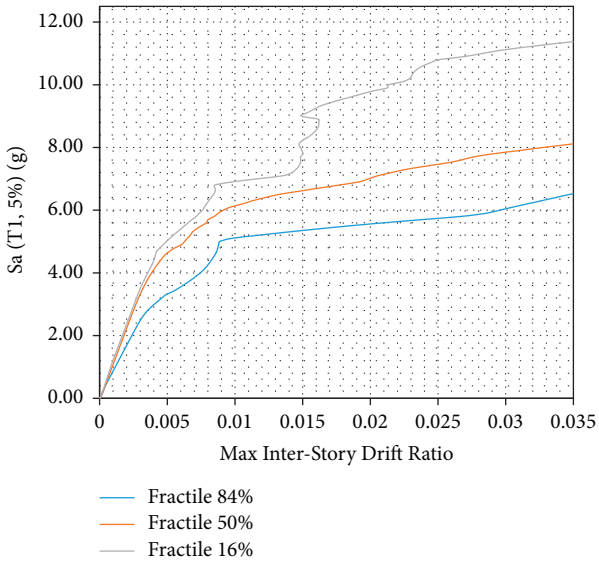

Figure 25: Fractile curves of the steel-HSS braced portal frame.

and 60 km as the boundaries of the near field. UBC-97 regulations provide a distance of fewer than 15 km from the center as the near area. But today it is commonly assumed that recorded movements less than 20 km from the fault location and the epicenter of the earthquake are near-fault maps. The characteristics of near-fault movements are directly related to the seismic source mechanism, the direction of fault rupture relative to the site, and the permanent changes in the ground at the site due to tectonic movements. These properties include the effect of rupture orientation, permanent deformation of the Earth, and high-frequency content. Somerville et al. [22] showed that the effects of orientation increase the response spectrum in periods longer than 0.6 seconds. To compare the response spectrum of near and far earthquakes, 15 ordinary earthquake maps were selected. Chopra et al. [23] found that near-fault effects have

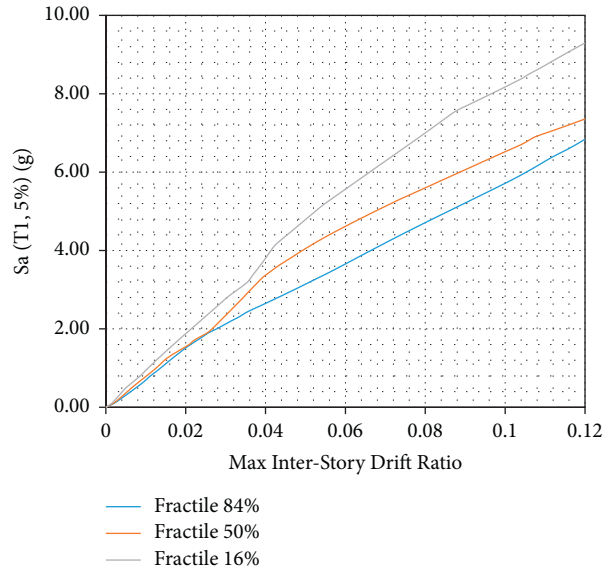

Figure 26: Fractile curves of the glulam braced portal frame.

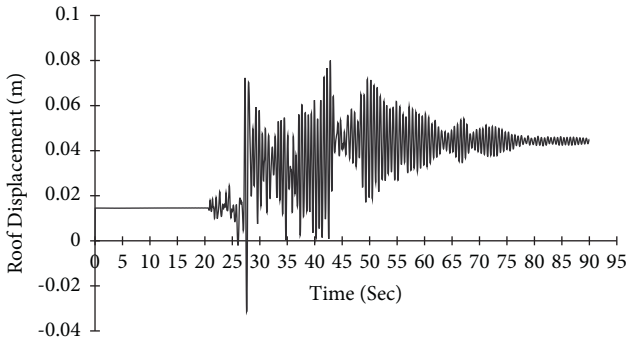

Figure 27: Displacement histories of the unbraced portal frame.

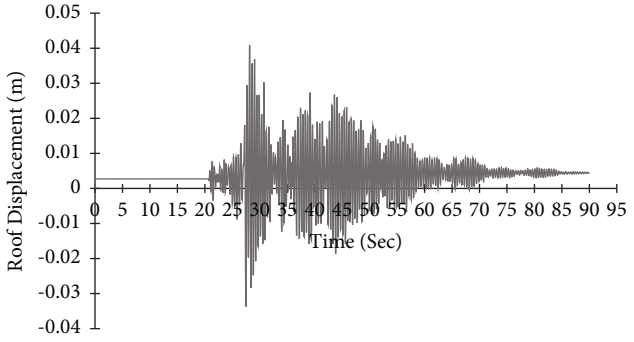

Figure 28: Displacement histories of the glulam braced portal frame.

significant influence on the quadratic response spectrum in a way that reduces the areas sensitive to velocity and increases the areas that are sensitive to displacement and acceleration.

4.6.1. Earthquakes Records for IDA and Time History Analysis. To more accurately evaluate the models in this study, it is necessary to simulate the time history analysis of

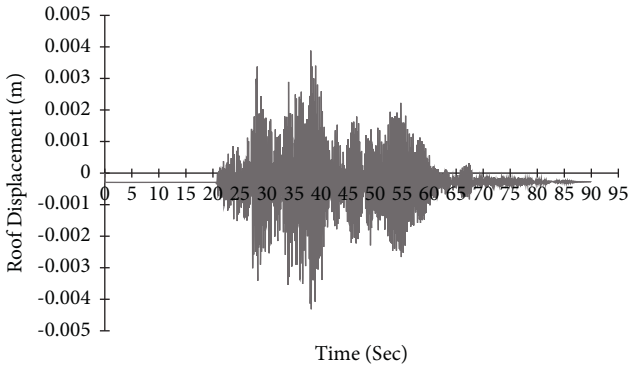

Figure 29: Displacement histories of the steel-HSS braced portal frame.

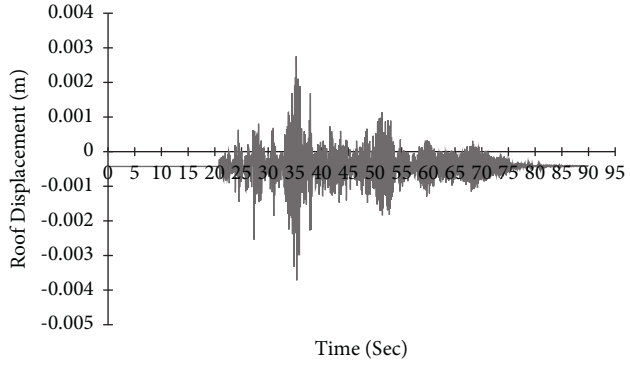

Figure 30: Displacement histories of the timber-steel-BRB frame.

the models using several ground acceleration records. For this purpose, seven seismic records to type C soil have been obtained from Pacific Earthquake Engineering Research Center. All records are from earthquakes with a magnitude of higher than 6.5 on the Richter scale. Table 8 shows the near-fault histories of type C soil, including peak ground acceleration (PGA) and earthquake magnitude. The selection of stories plays a very significant role in the results of time history analysis, and in the selection of records, in this paper, we used the results of studies conducted by Erol Kalkan et al. [24] in which Fling-Step and Forward-Rupture Directivity occurred. Acceleration response spectrum of selected records and their average are shown in Figure 31.

According to the results of the IDA curves, as shown in Figures 23–26, the portal steel frame without bracing has the maximum interstory drift. In steel-HSS and timber-steel-BRB braced frames, the maximum interstory drift is obtained for the values of constant seismic intensity. Also, in the case of using the steel-HSS brace, timber based glulam brace, and timber-steel-BRB, the maximum values of interstory drift occur at higher seismic intensities compared to the portal steel frame without bracing. Therefore, the use of steel-HSS brace, timber based glulam brace, and timber-steel-BRB has a significant impact on the reduction of the dynamic response of portal steel frame. The results show that the frame braced with the steel-HSS brace and the frame braced with timber based glulam brace have better seismic performance in reducing the maximum amount of interstory drift, increasing energy dissipation, and reducing the dynamic response. In general, it can be stated that, in all seismic intensities, in the cases of using timber based glulam, steel-HSS and timber-steel-BRB braces compared with portal steel frame without bracing, the demand values are reduced several times; this indicates the extra stiffness that the braces, steel-HSS, timber-steel-BRB, and timber based glulam, impose on the portal steel frame. The greatest reduction in seismic demand of interstory drift is in frame braced with timber-steel-BRB, and, as a result, timber-steel-BRB has the best energy dissipation and seismic performance. The occurrence of this optimal seismic performance can be due to symmetrical and stable hysteresis curves of buckling restrained braces that can experience the same capacities in tension and compression. Compared capacity and maximum interstory drift ratios (θ_{max}) of braced frames for immediate occupancy are listed in Tables 9–12.

4.7. Displacement History Investigation of Selected Portal Frames. To determine the seismic response of a structure under dynamic loading of the representative earthquake time history analysis is used [25]; another important issue in nonlinear time history analysis is damping. Equivalent viscous damping approach using Rayleigh formulation is commonly accepted. The damping matrix, C, is determined as follows:

$$C = \alpha m + \beta k. \tag{7}$$

In the above formula, m and k are the mass and stiffness matrices, respectively, and α and β are proportionality factors that are calibrated to result in a predefined percentage of critical damping (ξ) at two vibration periods. In time history analysis, the response of the building under the stimulation of actual earthquake histories is determined using dynamic relationships in short time. In this method, the response of the structure is based on at least three records. If less than seven records are selected for analysis, their maximum effect should be considered to control deformations and internal forces. If seven records or more are used, the average value of their effect can be considered to control deformations and internal forces [26]. Displacement history of portal frame is obtained in four conditions: without bracing, braced with steel-HSS, braced with timber based glulam, and braced with timber-steel buckling restrained brace (TS-BRB). Figures 27–30 are curves for roof node displacement histories of the portal steel frame without bracing, braced with steel-HSS, timber based glulam, and timber-steel buckling restrained brace (TS-BRB), respectively. The data from the time history analysis is under record number five, as shown in Table 8.

According to the results of time history analysis, as shown in Figures 27–30, the use of steel-HSS, timber based glulam, and timber-steel-BRB braces in the portal steel frame affects the history of displacement of the frame roof node. Therefore, the use of the steel-HSS brace, timber based glulam brace, and timber-steel-BRB brace has a significant effect on increasing energy dissipation, reducing the dynamic response of structures, and reducing the amount of

Table 7: Global interstory drift angle capacity C for regular SMF [21].

Building height	Performance level	
	Immediate occupancy Interstory drift angle capacity C	Collapse prevention Interstory drift angle capacity C
Low rise (3 stories or less)	0.02	0.1
Mid rise (4–12 stories)	0.02	0.1
High rise (>12 stories)	0.02	0.08

Table 8: Characteristics of selected records.

No.	T (sec)	Dt (sec)	Earthquake name	Year	Station	Magnitude (Richter)	PGA (g)
1	90	0.005	Chi-Chi-Taiwan	1999	TCU052	7.62	0.36
2	90	0.005	Chi-Chi-Taiwan	1999	TCU068	7.62	0.512
3	90	0.005	Chi-Chi-Taiwan	1999	TCU074	7.62	0.596
4	90	0.005	Chi-Chi-Taiwan	1999	TCU084	7.62	1.0
5	90	0.005	Chi-Chi-Taiwan	1999	TCU129	7.62	1.0
6	35	0.005	Kocaeli	1999	Yarimca (YPT)	7.51	0.23
7	25	0.005	Loma Prieta x	1989	LGPC	6.93	0.57

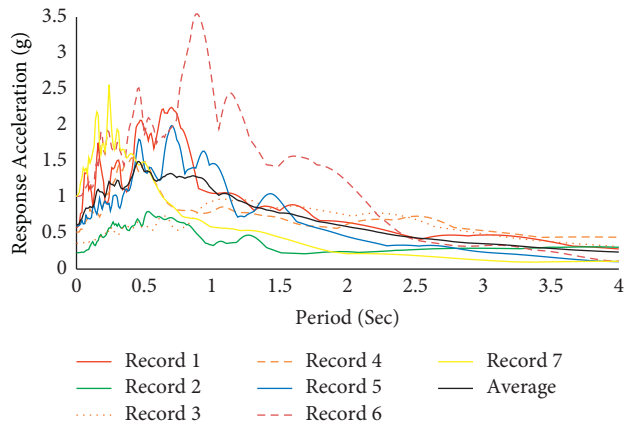

Figure 31: Acceleration response spectrum of selected records and their average.

Table 9: Summarized capacity of the unbraced portal frame for immediate occupancy (IO) limit state.

Fractile (%)	Type of frame	Sa (T1, 5%) (g)	θmax
16	Unbraced portal	0.8	0.02
50	Unbraced portal	0.7	0.02
84	Unbraced portal	0.6	0.02

Table 10: Summarized capacity of the steel-HSS braced portal frame for immediate occupancy (IO) limit state.

Fractile (%)	Type of frame	Sa (T1, 5%) (g)	θmax
16	Steel-HSS braced portal	9.7	0.02
50	Steel-HSS braced portal	7	0.02
84	Steel-HSS braced portal	5.6	0.02

residual displacement after the earthquake as summarized in Table 13.

The linear and nonlinear response of structures is greatly affected by the frequency content and basically in each earthquake record one or two components decomposed

Table 11: Summarized capacity of the glulam braced portal frame for immediate occupancy (IO) limit state.

Fractile (%)	Type of frame	Sa (T1, 5%) (g)	θmax
16	Glulam braced portal	1.8	0.02
50	Glulam braced portal	1.7	0.02
84	Glulam braced portal	1.6	0.02

Table 12: Summarized capacity of the timber-steel-BRB portal frame for immediate occupancy (IO) limit state.

Fractile (%)	Type of frame	Sa (T1, 5%) (g)	θMax
16	Timber-steel-BRB portal	11.6	0.02
50	Timber-steel-BRB portal	8.6	0.02
84	Timber-steel-BRB portal	7.6	0.02

from the record with a short frequency range (with a period close to the natural period of the structure) affecting the response of structures. This is why classifying records based on frequency content can be very useful for selecting the right accelerometer for time history analysis. In addition to the concentration of energy in frequency, the concentration of energy in time is also very important in the response of structures. The three main characteristics of an earthquake are amplitude, duration, and frequency content. There are different parameters to determine these three characteristics, some of which describe only one of the above three characteristics, while others describe two or even three characteristics. Parameters used to describe the amplitude of an earthquake include the peak ground acceleration (PGA), peak ground velocity (PGV), and peak ground displacement (PGD). Different methods are used to determine the duration of an earthquake, the most important of which is to determine the duration based on the ground acceleration, the intensity of the arias, and the acceleration of RMS. The dynamic response of structures is very sensitive to the loading frequency. Earthquakes create very complex loading in a frequency range. Therefore, the study of frequency

Table 13: Summery of maximum roof displacement history under selected record of different frames.

Type of portal steel frames	Brace effective area dimensions (mm)	Unit weight of brace length (kg/m)	Maximum roof displacement (m)
Steel-HSS braced	HSS $(60 \times 60 \times 3)$	5.18	0.0038
TS-BRB	(50×20)	7.85	0.0027
Glulam braced	(100×100)	4.5	0.04
Unbraced portal			0.08

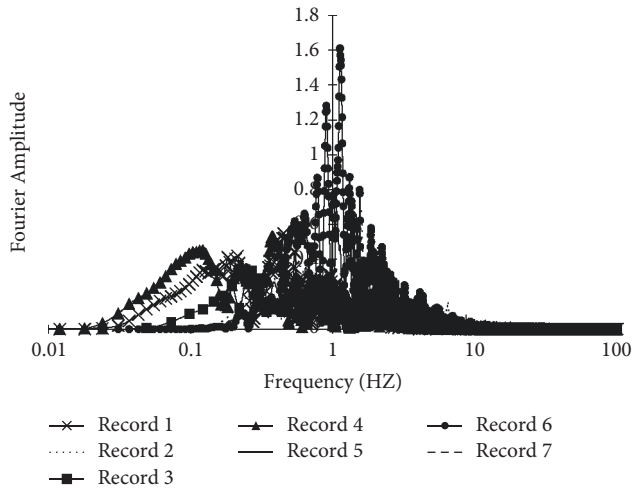

Figure 32: Fourier spectra of the seven studied earthquakes.

Table 14: Summary of decrease values in maximum roof displacement under selected record of different frames.

Type of portal steel frame	Brace effective area dimensions (mm)	Maximum roof displacement (m)	Decrease in maximum roof displacement (%)
Steel-HSS braced	HSS $(60 \times 60 \times 3)$	0.0038	95.2
TS-BRB	(50×20)	0.0027	96.6
Glulam braced	(100×100)	0.04	50
Unbraced		0.08	—

content is very important. In general, how the amplitude of the ground is distributed at different frequencies is called frequency content. The frequency information of earthquakes, unlike the amplitude and duration of the earthquake, cannot be extracted directly from the time history of the earthquake record, but this information is hidden, which requires various mathematical tools to extract it. The Fourier spectrum and the power spectrum are traditionally used to determine the frequency content of earthquakes. Fourier transform is a bridge between time and frequency which transmits the signal from the time domain to the frequency domain and extracts the signal information in the frequency domain. This type of conversion fails to determine the exact time of the different frequencies and can only determine the existence of the frequency. This type of frequency content expression is very useful for static signals. If the static signal has a frequency, that frequency is present in the whole time range. On the other hand, the time signals in earthquake engineering are inherently nonexistent in both frequency content and amplitude changes. In this study, to better extract the frequency information of the signals of seven selected records, their Fourier spectra are plotted in Figure 32.

5. Conclusions

The effect of using timber based bracings, Glued Laminated Timber (glulam), and timber-steel buckling restrained brace (TS-BRB) on seismic analysis of portal steel frames was investigated in this study; OpenSees FEM structural analyzer which is used for macromodeling is very simple and the time of modeling and analysis is short. The results of several seismic analysis strategies (such as pushover, cyclic, time history, and incremental dynamic analysis) on portal steel frames braced with timber based structural members (such as glulam and TS-BRB) are compared with similar portal steel frame behavior without or with steel bracing:

(i) According to the results of pushover analysis shown in Table 5, the frame without bracing has the lowest seismic capacity and the lowest amount of yield base shear. By adding timber based glulam, steel-HSS, and timber-steel-BRB braces, there is a considerable increase in base shear capacity equivalent to the first plastic hinge, 2.25, 6, and 7.93 times, respectively; this indicates the extra

shear capacity that the braces give to the unbraced portal steel frame.

(ii) Capacity curves of the frame braced with the steel-HSS brace and the frame braced with timber-steel-BRB brace show that the elastic stiffnesses (slope of the elastic region of the capacity curve) of the two types of braces are almost the same, but the equivalent yield base shear values and capacity of the frame braced with timber-steel-BRB are about 22.9% more compared to the frame braced with the steel-HSS brace. The frame braced with timber-steel-BRB has more stiffness than the frame braced with the steel-HSS so the frame braced with timber-steel-BRB can resist base shear more and has the best performance.

(iii) Compared to cyclic curves in Figures 19–22, it is concluded that the portal steel frame without bracing has the lowest surface area below the cyclic curve; it means that it has the lowest earthquake damping, resistance drop occurred in upper cycles, and also there are strength deteroiation and stiffness degradation. By adding timber base and steel braces, there is a considerable increase in energy dissipation and resistance drop did not occur in high cycles; also there is no strength and stiffness degradation. This indicates the extra stiffness and energy dissipation capacity that the braces, steel, glulam, and timber-steel-BRB, give to the unbraced portal steel frame.

(iv) Due to the elastic properties of the wood, the hysteresis curve of the glulam braced frame is thin.

(v) Compared to summarized IDA or fractile curves of 16%, 50%, and 84% from Tables 9–12 in general, it can be stated that, in all seismic intensities, in the cases of using timber based glulam, steel-HSS, and timber-steel-BRB braces in portal steel frame, the demand values are reduced several times; this indicates the extra lateral strength that the braces, steel-HSS, timber based glulam, and timber-steel-BRB, give to the portal steel frame.

(vi) Comparison of 16% summarized IDA curves shows that the interstory drift of 0.02 in the unbraced portal frame is obtained in spectral acceleration corresponding to the first model of the structure with 5% damping of 0.8 g, but with the addition of wooden glulam brace this interstory drift is obtained in 1.8 g; this indicates 1 g extra intensity measure capacity. Using glulam brace has a significant role in the control of interstory drift compared to its weight.

(vii) Compared to displacement histories obtained from time history analysis, using steel-HSS, timber based glulam, and timber-steel-BRB braces in the portal steel frame, the decrease in maximum roof displacement is 95%, 50%, and 96.6%, respectively, This indicates a significant effect of braces on the displacement control of the roof node as summarized in Table 14.

(viii) In timber-hybrid structures steel is strong with significant postyield deflection capability, known as ductility; timber is comparatively weaker, usually requiring larger sections, resulting in stiffer systems; wood does not produce postyield deflection, especially when loaded perpendicular to the grain.

(ix) Hybrid timber-steel-BRB frames counteract the negative postyield stiffness that occurs due to P-Delta effects. They are more effective on buildings where P-Delta effects are more critical.

(x) The repair costs of the structures with hybrid timber-steel-BRB frames will be less due to lower residual drifts.

(xi) Due to low density of wood by using timber based braces, there is a considerable reduction in the frame weight corresponding to its strength.

(xii) The results of the analysis showed that glulam can withstand different dynamic loads as a brace and confinement of the buckling restrained brace in hybrid timber-steel structures, in which case there is a significant reduction in the weight and cost of estimation of the structure.

Data Availability

The data used to support the findings of this study are available from the corresponding author upon request.

Conflicts of Interest

The authors declare that they have no conflicts of interest regarding the publication of this paper.

Acknowledgments

The authors thank Professors of the Civil Engineering Department, K. N. Toosi University of Technology, for their complete guidance in this research and also thank the laboratory officials of this university for their cooperation in getting experimental data for numerical modeling.

References

[1] M. Moore, "Scotia place – 12 story apartment building. A case study of high-rise construction UsingWood and steel," *NZ Timber Design journal*, vol. 10, no. 1, pp. 5–12, 2000.

[2] C. Gilbert, R. Gohlich, and J. Erochko, "Nonlinear Dynamic Analysis of Innovative High R-Factor Hybrid Timber-Steel Buildings," in *Proceedings of the 11th Canadian Conference of Engineering*, Victoria, Canada, July 2015.

[3] C. Gilbert and J. Erochko, "Adaptation of Advanced High R-Factor Bracing Systems into Heavy Timber Frames," in *Proceedings of the World conference of timber engineering*, Vienna, Austria, Aguest 2016.

[4] M. Timmers and A. Tsay Jacobs, "Concrete apartment tower in Los Angeles reimagined in mass timber," *Engineering Structures*, vol. 167, pp. 716–724, 2018.

[5] S. R. S. Monteiro, C. Martins, A. M. P. G. Dias, and H. Cruz, "Mechanical performance of glulam products made with

Portuguese poplar," *European Journal of Wood and Wood Products*, vol. 78, no. 5, pp. 1007–1015, 2020.

[6] H. E. Blomgren and J. P. Koppitz, "Heavy timber buckling-restrained braced frame as solution for commercial buildings," in *Proceedings of the World Conference on Timber Engineering*, Vienna, Austria, August 2016.

[7] D. G. Lignos and H. Krawinkler, "Deterioration modeling of steel components in support of collapse prediction of steel moment frames under earthquake loading," *Journal of Structural Engineering*, vol. 137, no. 11, pp. 1291–1302, 2011.

[8] P. C. Hsiao, D. E. Lehman, and C. W. Roeder, "Improved analytical model for special concentrically braced frames," *Journal of Constructional Steel Research*, vol. 73, no. 2, pp. 80–94, 2012.

[9] D. C. Antonio, C. P. Nicla, and N. Domenico, "Modeling of post-tensioned timber framed buildings with hysteretic bracing system," *IOP Conference Series: Earth and Environmental Science*, vol. 233, no. 2, pp. 1–10, 2019.

[10] O. Atlayan and F. A. Charney, "Hybrid buckling-restrained braced frames," *Journal of Constructional Steel Research*, vol. 96, pp. 95–105, 2014.

[11] L. Jiun-Wei and S. A. Stephen, "Experimental and Analytical Studies on the Seismic Behavior of Conventional and Hybrid Braced Frames," *UC Berkeley Electronic Theses and Dissertations, Civil and Environmental Engineering Faculty*, University of California, Berkeley, 2013.

[12] M. Popovski, H. G. L. Prion, E. Karacabeyli, and E. Karacabeyli, "Shake table tests on single-storey braced timber frames," *Canadian Journal of Civil Engineering*, vol. 30, no. 6, pp. 1089–1100, 2003.

[13] P. Kaley and A. M. Baig, "Pushover analysis of steel framed building," *Journal of Civil Engineering and Environmental Technology*, vol. 4, no. 3, pp. 301–306, 2017.

[14] P. Fema-356, *Pre-standard and Commentary for the Seismic Rehabilitation of Buildings*, Federal Emergency Management Agency, Washington, DC, USA, 2000.

[15] P. Panyakapo, "Cyclic Pushover Analysis procedure to estimate seismic demands for buildings," *Engineering Structures*, vol. 66, pp. 10–23, 2014.

[16] Applied Technology Council (Atc-24), *Guidelines for Cyclic Testing of Components of Steel Structures*, Applied Technology Council, Redwood City, CA, 1992.

[17] An American National Standard ANSI/AISC 341-05Seismic Provisions for Structural Steel Buildings, Chicago, IL, USA, 2005.

[18] D. Vamvatsikos and C. A. Cornell, "Applied incremental dynamic analysis," *Earthquake Spectra*, vol. 20, no. 2, pp. 523–553, 2004.

[19] D. Vamvatsikos and C. A. Cornell, "Incremental dynamic analysis," *Earthquake Engineering & Structural Dynamics*, vol. 31, no. 3, pp. 491–514, 2002.

[20] D. Vamvatsikos and C. Allin Cornell, "Direct estimation of the seismic demand and capacity of oscillators with multi-linear static pushovers through IDA," *Earthquake Engineering & Structural Dynamics*, vol. 35, no. 9, pp. 1097–1117, 2006.

[21] A. K. Chopra and F. McKenna, "Modeling viscous damping in nonlinear response history analysis of buildings for earthquake excitation," *Earthquake Engineering & Structural Dynamics*, vol. 45, no. 2, pp. 193–211, 2016.

[22] P. G. Somerville, N. F. Smith, R. W. Graves, and N. A. Abrahamson, "Modification of empirical strong ground motion attenuation relations to include the amplitude and duration effects of rupture directivity," *Seismological Research Letters*, vol. 68, no. 1, pp. 199–222, 1997.

[23] A. K. Chopra and C. Chintanapakdee, "Drift spectrum vs. Modal analysis of structural response to near-fault ground motions," *Earthquake Spectra*, vol. 17, no. 2, pp. 221–234, 2001.

[24] E. Kalkan and S. K. Kunnath, "Effects of fling step and forward directivity on seismic response of buildings," *Earthquake Spectra*, vol. 22, no. 2, pp. 367–390, 2006.

[25] P. C. Nguyen, "Nonlinear inelastic earthquake analysis of 2D steel frames," *Engineering, Technology & Applied Science Research*, vol. 10, no. 6, pp. 6393–6398, 2020.

[26] B. Mohraz, "A study of earthquake response spectra for different geological conditions," *Bulletin of the Seismological Society of America*, vol. 66, no. 3, pp. 915–935, 1976.